

## Effects of Ga ions on some properties of Lithium zinc nanocrystallines $\text{Li}_{0.35}\text{Zn}_{0.3}\text{Fe}_{2.35-x}\text{Gd}_x\text{O}_4$

Yun He<sup>1</sup>, Kaimin Su<sup>1</sup>, Zhiqing Luo<sup>1</sup>, Hangyu Xu<sup>1</sup>, Zhimin Ji<sup>1</sup>, Jinpei Lin<sup>1</sup>,  
Yunlong Wang<sup>1</sup> and Qing Lin<sup>1,2,a</sup>

<sup>1</sup>College of Physics and Technology, Guangxi Normal University, Guilin 541004, China

<sup>2</sup>College of Medical Informatics, Hainan Medical University, Haikou 571199, China

**Keywords:** Lithium zinc nanocrystallines

**Abstract.** Polycrystalline samples  $\text{Li}_{0.35}\text{Zn}_{0.3}\text{Fe}_{2.35-x}\text{Gd}_x\text{O}_4$  ( $x=0, 0.02, 0.04, 0.06, 0.08, 0.10$ ) were prepared by sol-gel auto-combustion method. The XRD analysis shows that the samples are cubic spinel ferrite, the lattice parameter increased and the average grain size decreased with  $\text{Gd}^{3+}$  ions concentration increasing. The quadrupole splitting reflects the degree of charge deviating from the symmetrical distribution of local area around the Mössbauer nuclear  $\text{Fe}^{3+}$ . So the charge around the  $\text{Fe}^{3+}$  tends to symmetrical distribution in this serie of samples, and the distribution is almost not affected by the  $\text{Gd}^{3+}$  doping.

### Introduction

The magnetism of rare earth elements comes from the 4f electrons, which screened by the outer shell of the  $5s^25p^6$  electrons, giving rise to special electromagnetic properties of rare earth atoms and ions [1-2]. Adding a certain amount of rare earth elements to the ferrite magnetic material, the rare earth ions and the transition element ions in ferrite produce 4f-3d electron exchange effect, has a remarkable decoration effect to the structure of ferrite, becoming one of the important ways to improve the performance [3-4]. The magnetic moment of the rare earth ions has a wide variation range from 0 to  $10.6 \mu_B$ . However, their Curie temperatures are generally low, thus the magnetism is hardly shown under the normal temperature environment. Gadolinium is the only one rare earth element whose Curie temperature closing to room temperature. The 4f electronic shell of  $\text{Gd}^{3+}$  ions is half full, resulting in a large magnetic moment. And the radius is relatively large ( $0.0938 \text{ nm}$ ), making the  $\text{Gd}^{3+}$  ions have a strong tendency to occupy the octahedral site (B) when they are added into the spinel ferrite [5-7]. Doped with a small amount of  $\text{Gd}^{3+}$  ions is expected to enhance the magnetism of lithium zinc ferrite. In this paper, polycrystalline samples  $\text{Li}_{0.35}\text{Zn}_{0.3}\text{Fe}_{2.35-x}\text{Gd}_x\text{O}_4$  ( $x=0, 0.02, 0.04, 0.06, 0.08, 0.10$ ) were prepared by sol-gel auto-combustion method. The main purpose is to investigate the effect of substitution of gadolinium on microstructural and magnetic properties of lithium zinc ferrite.

### Experimental

#### Sample preparation

Samples were prepared by sol-gel auto-combustion method. Experiment preparation process is shown in Figure 1:

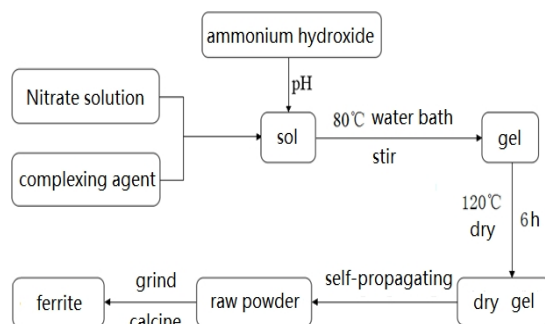


Figure 1. The preparation process of  $\text{Li}_{0.35}\text{Zn}_{0.3}\text{Fe}_{2.35-x}\text{Gd}_x\text{O}_4$  powder

Specific operation is as follows:

- The analytical grade  $\text{LiNO}_3$ ,  $\text{Zn}(\text{NO}_3)_2 \cdot 6\text{H}_2\text{O}$ ,  $\text{Fe}(\text{NO}_3)_3 \cdot 9\text{H}_2\text{O}$ ,  $\text{Gd}(\text{NO}_3)_3 \cdot 6\text{H}_2\text{O}$  were accurately weighed according to the stoichiometric ratio  $\text{Li}_{0.35}\text{Zn}_{0.3}\text{Fe}_{2.35-x}\text{Gd}_x\text{O}_4$ , and dissolved thoroughly into deionized water.
- The analytical grade citric acid ( $\text{C}_6\text{H}_8\text{O}_7 \cdot \text{H}_2\text{O}$ ) was added into the mixed solution. And the molar ratio of citric acid to total metal nitrates ( $n(\text{CA}):n(\text{M})$ ) was taken as 1:1.
- The mixed solution was added Ammonia to adjust the pH value to 7.
- Put the beakers which contained the sol into thermostat water baths and heated at  $80^\circ\text{C}$  along with constant stirring until transform into gel.
- After 12h of aging time, the wet gel were put into a electrothermal blowing dry box and dried at  $120^\circ\text{C}$  for 6h, transforming into dry gel.
- Took out a little dry gel to make thermogravimetric test. Dropped a little absolute ethyl alcohol on the rest of it. Being ignited in aria at indoor temperature, the dry gel occurred a self-propagating reaction, formed fluffy flocculent substance.
- After fully ground in a agate mortar, fine powders were obtained. Annealed the powders in a muffle furnace at temperatures  $800^\circ\text{C}$  for 2h. Samples of target were obtained after natural cooling.

### Characterizations

The thermal decomposition behavior of gel was analyzed by thermal analysis instrument (SDT Q600, America). The crystalline structure of sample was performed using X-ray diffraction (D8 Advance, Germany) with  $\text{Cu K}\alpha$  radiation ( $\lambda=0.15405\text{nm}$ ). The microstructure of particles was observed by scanning electron microscope (SU8020, Japan). The Mössbauer spectra were performed using conventional Mössbauer spectrometer (Fast Com Tec PC-moss II, Germany) at room temperature, in constant acceleration mode. The  $\gamma$ -ray was provided by a  $^{57}\text{Co}$  source in a rhodium matrix.

## Results and discussion

### TG-DSC analysis

TG, DTG and DSC curves for the dry gel of  $\text{Li}_{0.35}\text{Zn}_{0.3}\text{Fe}_{2.35}\text{O}_4$  are presented in Figure 2. As shown in the picture, the system loss about 12.5% of the weight before the temperature of  $196^\circ\text{C}$ , because of the evaporation of the remaining molecular water and crystal water [8-9].

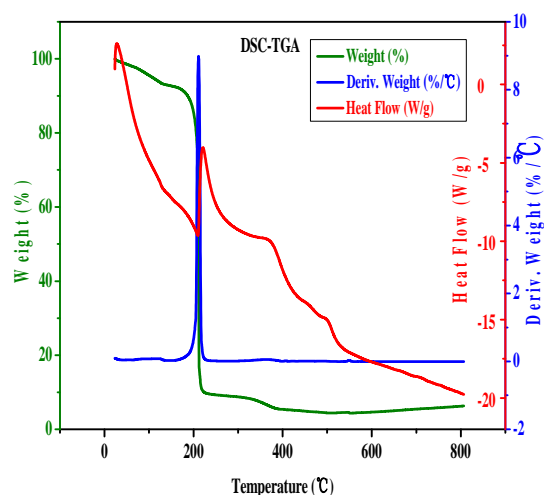


Figure 2. TG-DSC curves for the dry gel of  $\text{Li}_{0.35}\text{Zn}_{0.3}\text{Fe}_{2.35}\text{O}_4$

Correspondingly, there is an endothermic peak on the DSC curve near this temperature. From about 203.2°C to 216.7°C, the weight loss of the system is nearly 76.3%, with a sharp exothermic peak locating in the vicinity of about 220.8°C. This phenomenon corresponds to the decomposition reaction of citrates and nitrate in the gel. The reaction is a kind of self oxidation-reduction reaction which releases great heat[10,11]. Whereafter, the system loss about 6.1% of the weight from about 217.1°C to 369.6°C, with a subdued exothermic peak locating in the vicinity of about 370°C, corresponding to the crystallization process of the system[12,13]. After this, the system stays almost invariant weight, and forms a relatively stable phase after 550°C. With temperature increasing, the weight of the system increases slowly, the corresponding grain will continue to grow. In consideration of time-delay effect caused by the heating rate of 10°C/min, the crystalline temperature should be slightly lower than 550°C.

### XRD analysis

Figure 3 shows the XRD patterns of  $\text{Li}_{0.35}\text{Zn}_{0.3}\text{Fe}_{2.35-x}\text{Gd}_x\text{O}_4$  ferrite powders calcined at 550°C for 2h. Compared with the standard patterns given in International Centre for Diffraction Data (ICDD) files, the XRD patterns all exhibit cubic spinel structure of  $\text{Li}_{0.435}\text{Zn}_{0.195}\text{Fe}_{2.37}\text{O}_4$  (file no: PDF#37-1471, space group  $\text{Fd}3\text{m}$ ). No impurity peak is detected in these samples. In the range of 20~70°, the main diffraction peaks of this XRD patterns are (220), (311), (222), (400), (422), (511) and (440), whereby the diffracted intensity of the diffraction peak of (311) is maximum[14]. The actual phases of gadolinium doped lithium zinc ferrites are different from the expected results, possibly because lithium, zinc and the corresponding compounds produce some extent of volatility during self propagating process and the subsequent calcination process [15,16].

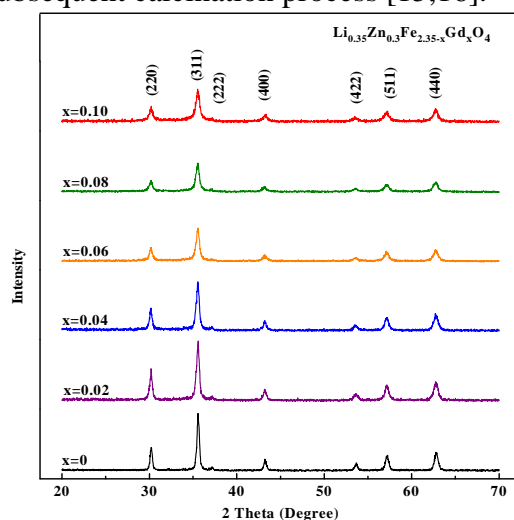


Figure 3. XRD of  $\text{Li}_{0.35}\text{Zn}_{0.3}\text{Fe}_{2.35-x}\text{Gd}_x\text{O}_4$  ferrites

Figure 4 shows the drifting of the main diffraction peaks of  $\text{Li}_{0.35}\text{Zn}_{0.3}\text{Fe}_{2.35-x}\text{Gd}_x\text{O}_4$ . It can be seen from the graph that with an increasing amount of gadolinium content, the diffraction peaks get broader and broader, whilst the position of the peaks have no obvious change. According to Scherrer Equation:  $D = \frac{Kl}{b \cos \theta}$ , increasing of the full width at half maximum (FWHM) of the diffraction peak stands for a decreasing of average crystallite size. Table 1 shows the average crystallite size, lattice parameters, X-ray densities date of  $\text{Li}_{0.35}\text{Zn}_{0.3}\text{Fe}_{2.35-x}\text{Gd}_x\text{O}_4$  after cell refinement.

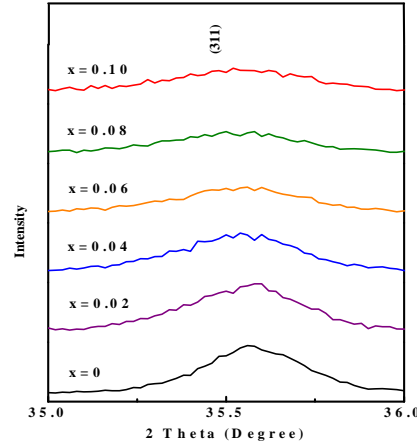


Figure 4. Drifting of the main diffraction peaks

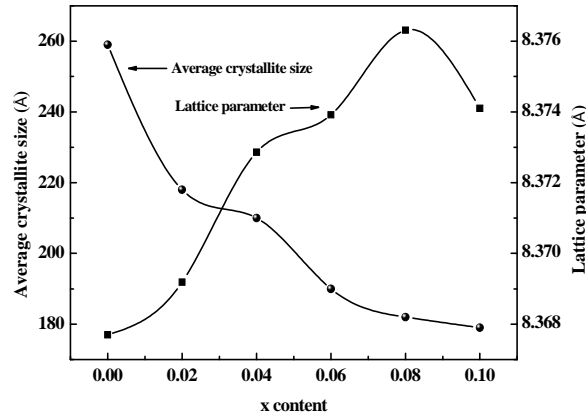


Figure 5. The average crystallite size and lattice parameter of  $\text{Li}_{0.35}\text{Zn}_{0.3}\text{Fe}_{2.35-x}\text{Gd}_x\text{O}_4$

**Table 1.** The XRD datum of  $\text{Li}_{0.35}\text{Zn}_{0.3}\text{Fe}_{2.35-x}\text{Gd}_x\text{O}_4$  ferrites

Sample (x)	Average crystallite size (Å)	Lattice parameter (Å)	Density ( $\text{g}\cdot\text{cm}^{-3}$ )
0	259	8.367	4.926
0.02	218	8.369	4.969
0.04	210	8.372	5.008
0.06	190	8.373	5.052
0.08	182	8.376	5.094
0.10	179	8.374	5.144

Figure 5 visualizes the relationship between the XRD parameters and gadolinium doping content. With the increment of  $\text{Gd}^{3+}$  doping, the average crystallite size of sample presents a tendency of decreasing. According to the density of X-ray diffraction formula  $\rho_x = \frac{8M}{Na^3}$ , the theoretical density of samples will gradually increase.

## SEM analysis

The SEM micrographs of  $\text{Li}_{0.35}\text{Zn}_{0.3}\text{Fe}_{2.35-x}\text{Gd}_x\text{O}_4$  ( $x=0, 0.04, 0.10$ ) ferrites calcined  $550^\circ\text{C}$  for 2h and their particle size distribution histogram are shown in Figure 6. It can be observed from the SEM micrographs that the particle size distribution is almost uniform, and the crystallinity of the samples is relatively well. Magnetic interaction force between particles is difficult to avoid, making samples in some extent of agglomeration[10]. Agglomeration in the samples of high  $\text{Gd}^{3+}$  content is relatively weak, this may attribute to the magnetic interaction in these samples is relatively weak. Analysed by the statistical method, the average particle size of the sample of  $\text{Li}_{0.35}\text{Zn}_{0.3}\text{Fe}_{2.35}\text{O}_4$ ,  $\text{Li}_{0.35}\text{Zn}_{0.3}\text{Fe}_{2.31}\text{Gd}_{0.04}\text{O}_4$ ,  $\text{Li}_{0.35}\text{Zn}_{0.3}\text{Fe}_{2.25}\text{Gd}_{0.10}\text{O}_4$  is 43.64 nm, 32.29 nm and 29.55 nm, respectively. This shows that along with the increasing of  $\text{Gd}^{3+}$  content, the average particle size of sample decreases, and all the samples belong to the nanoparticles. The average particle sizes are larger than the corresponding XRD grain sizes, because the sample of each particle is composed of a number of grains[11].

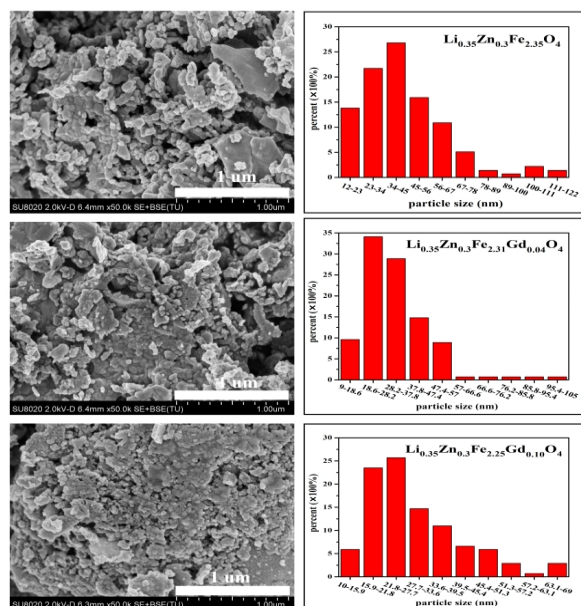


Figure 6. SEM micrographs of  $\text{Li}_{0.35}\text{Zn}_{0.3}\text{Fe}_{2.35-x}\text{Gd}_x\text{O}_4$

## Mössbauer spectrum analysis

Figure 7 shows the room temperature Mössbauer spectra of  $\text{Li}_{0.35}\text{Zn}_{0.3}\text{Fe}_{2.35-x}\text{Gd}_x\text{O}_4$  ( $x=0, 0.04, 0.10$ ) calcined at  $550^\circ\text{C}$  for 2h. Table 2 shows the related parameters fitted by Mösswinn 3.0 programme. Isomer shift in the range of 0.1~0.5 mm/s, according to the literature [12], iron ions in this series of samples are all  $\text{Fe}^{3+}$ . The nearest neighbor A sites of  $\text{Fe}^{3+}$  in B sites are occupied by  $\text{Zn}^{2+}$  probabilistically, thus magnetic hyperfine field in B sites presents a distribution, giving rise to the line broadening. The amount of  $\text{Fe}^{3+}$  in B sites decreases by increasing  $\text{Gd}^{3+}$  substitution. The absorption area in B sites decreases by increasing  $\text{Gd}^{3+}$  substitution. In accordance with the discussion above, the magnetic dipole orientation of  $\text{Gd}^{3+}$  presents a disordered state in room temperature which higher than the Curie temperature. The spectra of sample of  $x=0.04$  exhibits two Zeeman-split sextets and a paramagnetic doublet. The paramagnetic doublet roots in the paramagnetism of sample and the superparamagnetism caused by the small size particles. The proportion of paramagnetic spectrum in sample of  $x=0.10$  has significantly enhanced, due to the magnetism is weaker and the average particle size is smaller. The quadrupole splitting of the serie of samples are all small. Thus the doping will weaken the magnetism of the sample, make the sample transform from ferrimagnetic state to paramagnetic state.

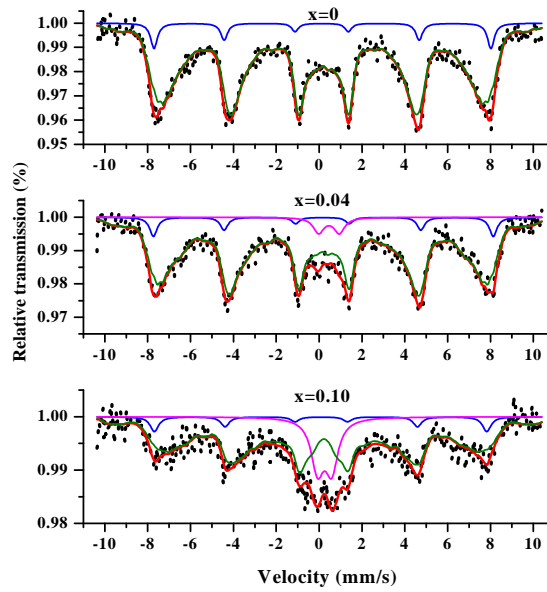


Figure 7. Room temperature Mössbauer spectra of  $\text{Li}_{0.35}\text{Zn}_{0.3}\text{Fe}_{2.35-x}\text{Gd}_x\text{O}_4$

**Table 2.** The Mössbauer spectra of  $\text{Li}_{0.35}\text{Zn}_{0.3}\text{Fe}_{2.35-x}\text{Gd}_x\text{O}_4$

Sample (x)	Component	IS (mm/s)	QS (mm/s)	$\Gamma$ (mm/s)	$A_0$ (%)
0	Sextet (A)	0.138	0.038	0.380	6.50
	Sextet (B)	0.198	-0.043	0.411	93.5
0.04	Sextet (A)	0.177	0.041	0.422	6.20
	Sextet (B)	0.193	-0.067	0.410	90.2
	Double	0.460	0.964	0.598	3.50
0.10	Sextet (A)	0.083	-0.032	0.469	6.10
	Sextet (B)	0.198	-0.058	0.455	78.1
	Double	0.257	0.660	0.715	15.7

## Conclusions

In this paper, we compose a series of  $\text{Gd}^{3+}$  doped lithium zinc ferrite  $\text{Li}_{0.35}\text{Zn}_{0.3}\text{Fe}_{2.35-x}\text{Gd}_x\text{O}_4$  ( $x=0,0.02,0.04,0.06,0.08,0.10$ ) nano-particles via sol-gel auto-combustion method. TG and DSC analysis obtains that the best calcining temperature in this series samples is 550 °C. The XRD analysis showed that the samples are cubic spinel ferrite, the lattice parameter increased and the average grain size decreased with  $\text{Gd}^{3+}$  ions concentration increasing. The Mössbauer Spectrum analysis showed that ferromagnetic phase gradually transformed into a paramagnetic phase with  $\text{Gd}^{3+}$  ions concentration increasing.

## Acknowledgments

This work was supported by the National Natural Science Foundation of China (NO.11364004, 11164002); Graduate student excellent thesis cultivation plan of Guangxi Normal University (NO.A410213000001).

## References

1. M. De Marco, X.W. Wang, R.L. Snyder, J. Simmins, S. Bayya, M. White, M.J. Naughton. *Journal of applied physics*, 1993, 73(10): 6287-6289.
2. A.I. Borhan, T. Slatineanu, A.R. Iordan, M.N. Palamaru. *Polyhedron*, 2013, 56: 82-89.
3. A.I. Ali, M.A. Ahmed, N. Okasha, M. Hammam, J.Y. Son. *Journal of Materials Research and Technology*, 2013, 2(4): 356-361.
4. N. Rezlescu, E. Rezlescu, P.D. Popa, L. Rezlescu. *Journal of alloys and compounds*, 1998, 275: 657-659.
5. Zhang Y, Wen D. *Journal of the American Ceramic Society*, 2012, 95(9): 2919-2927.
6. R. Islam, M.A. Hakim, M.O. Rahman, H.N. Das, M.A. Mamun. *Journal of Alloys and Compounds*, 2013, 559, 174-180.
7. R.P. Pant, M. Arora, B. Kaur, V. Kumar, A. Kumar. *Journal of Magnetism and Magnetic Materials*, 2010, 322(22), 3688-3691.
8. G. Dixit, J.P. Singh, R.C. Srivastava, et al. *Journal of Magnetism and Magnetic Materials*, 2012, 324(4), 479-483.
9. J. Peng, M. Hojamberdiev, Y. Xu, B. Cao, J. Wang, H. Wu. *Journal of Magnetism and Magnetic Materials*, 2011, 323(1): 133-137.
10. M.V. Chaudhari, S.E. Shirsath, A.B. Kadam, R.H. Kadam, S.B. Shelke, D.R. Mane. *Journal of Alloys and Compounds*, 2013, 552: 443-450.
11. M.F. Al-Hilli, S. Li, K.S. Kassim. *Journal of Magnetism and Magnetic Materials*, 2012, 324(5), 873-879.
12. S. Amiri, H. Shokrollahi. *Journal of Magnetism and Magnetic Materials*, 2013, 345: 18-23.
13. A. Rana, O.P. Thakur, V. Kumar. *Materials Letters*, 2011, 65(19): 3191-3192.
14. M.A. Ahmed, H.H. Afify, I.K. El Zawawia, A.A. Azab. *Journal of Magnetism and Magnetic Materials*, 2012, 324(14): 2199-2204.
15. S.A. Mazen, N.I. Abu-Elsaad. *Journal of Magnetism and Magnetic Materials*, 2012, 324(20), 3366-3373.
16. D.H. Ridgley, H. Lesoff, J.D. Childress. *Journal of the American Ceramic Society*, 1970, 53(6), 304-311.